Discover Materials

Discover

Review

Review on light absorbing materials for unassisted photoelectrochemical water splitting and systematic classifications of device architectures

Choongman Moon[1] · **Byungha Shin**[1]

Received: 13 April 2022 / Accepted: 13 May 2022
Published online: 23 May 2022

Abstract
A photoelectrochemical (PEC) water-splitting device integrates a photovoltaic cell and electrocatalysts into a single device to produce hydrogen fuel from water using solar irradiance. The major driving force behind PEC research is that it can potentially be a cost-efficient way to produce hydrogen in a renewable way, however, current PEC devices for hydrogen production are not economically viable yet. This review provides comprehensive discussions on the major challenges on practical solar hydrogen production by PEC from the standpoint of device structure and light absorber materials. We started by systematically classifying PEC device structures based on the electrical junctions on the light absorber materials. Based on the classification scheme, we showed that the choices of a device structure and light absorber materials are cross-linked in current PEC studies and affects electron/ion transport in a PEC device. The correlation between the device structure and materials underlines the necessity of reviewing the light absorber materials for the top and bottom cells in a tandem PEC device as a whole. We categorize the light absorber materials based on their crustal abundance because it is a major factor that determines device structure and scalability in TW-scale, and discuss their influence on the efficiency, stability, and scalability of a PEC water-splitting system.

1 Introduction

Global consensus [1, 2] on regulating carbon emission via the transition from fossil fuels to alternative emission-free energy carriers has been reached to mitigate climate change. One of the most promising clean energy carriers is hydrogen because it releases only water during its combustion and can be in principle produced from water using renewable energy sources without greenhouse gas emissions. With the recent advances in solar cell technology, connecting a photovoltaic (PV) cell and electrocatalyst (EC) for solar hydrogen production is being considered as a potentially viable option. Nevertheless, industrial solar hydrogen production by the combination of PV and EC still requires significant developments and policy-level supports because the cost of hydrogen production by the PV + EC is still much higher than fossil fuel-based technologies such as steam methane reforming [3].

Photoelectrochemical (PEC) water splitting device integrates PV and EC into a single concise structure to make solar hydrogen production more feasible. In a PEC device structure, a semiconductor light absorber is immersed in an electrolyte with EC on its surface, and the photovoltage generated from the light absorber drives the electrochemical water splitting reaction directly over the surface. Because the photocurrent is distributed over the large surface of the solar

✉ Byungha Shin, byungha@kaist.ac.kr | [1]Department of Materials Science and Engineering, Korea Advanced Institute of Science and Technology (KAIST), Daejeon 34141, Republic of Korea.

cell rather than concentrated into a separate water electrolyzer, PEC device can operate at a much lower current density (10–20 mA/cm^2) than water electrolyzer (1–2 A/cm^2), and it results in a lower loss by an electrochemical overpotential from water-splitting catalysts [4]. In addition, photoexcited charge carriers from a PEC device participate in the electrochemical reaction on-site, whereas those from a conventional PV cell have to travel across its large surface and through a wire connection to the EC in the electrolyte. Therefore, PEC devices do not suffer from the ohmic loss from a transparent conductive oxide (TCO) and the wiring between PV-EC, and they also do not require an additional process for surface metallization. This advantage becomes more pronounced when considering the scale-up of the PEC devices for practical solar hydrogen production. Furthermore, the concise PEC device structure can potentially lower the system cost. PEC devices do not need electrodes which are necessary in a water electrolyzer (bipolar plate and porous transport layers), surface metallization necessary for a PV cell (metal grid contact) and power electronics needed for combining PV and EC (AC-DC or DC-DC inverter).

To take these advantages, various types of PEC devices, which usually consist of two or more semiconductor light absorbers with different bandgaps to enable unassisted (i.e., with no external power) water splitting, have been investigated. The construction of the PEC devices requires contacts between the semiconductor and an electrolyte, that is a solid–liquid junction (SLJ), or between the semiconductor and an external electrical circuit by a solid-state junction (SSJ). How to establish the connections through the junctions is an important factor to be considered when designing a PEC device structure. Another important factor is the choice of semiconductor light absorbers because the physical/chemical properties of the semiconductors affect the activity, stability and scalability of a PEC device. In this review, we introduce a systematic classification of PEC devices based on their electrical junctions and discuss which configurations would be beneficial to fully utilize the advantages of PEC. Furthermore, we will also review semiconductor light absorbers materials that have been adopted in various PEC structures and discuss their strengths and weaknesses. Over the course of our discussions, we also point out major challenges of PEC that should be addressed to realize practical solar hydrogen production. We expect that this comprehensive review of the device structure, materials and other critical issues will help guide the direction where research efforts should be focused.

2 Systematic classification of PEC device structures

For the extraction of useful work from a semiconductor light absorber under illumination, photogenerated charge carriers should be extracted through electrical junctions on its front and backside. Conventional PV cells extract charge carriers through SSJ's (also called a terminal), and the device structure is often named after the number of SSJ's—for example, "two-terminal" or "three-terminal" devices. On the other hand, PEC devices replace at least one of SSJ's with a SLJ to drive the water-splitting reaction over its surface, and one can devise many different designs depending on how to replace SSJ's with SLJ's. For example, a PEC device consisting one semiconductor with a SLJ on one side and a SSJ on the other is usually called as "photocathode" [5–9] or "photoanode" [10–15] depending on the type of charges involved in the reaction at the SLJ. A tandem PEC device, which comprises two semiconductors, are referred as "wired tandem" when connecting a photocathode and a photoanode with an electrical wire (two SLJ and two SSJ), or as "wireless tandem" when integrating the two semiconductors by a recombination layer between them, i.e., two SLJ's and a recombination layer [16–18]. Many alterations to the aforementioned PEC structures have been demonstrated, and the previous works attempt to classify the structures in the order of "design complexity" [17], or "topological variation of a device structure between PV + EC and PEC" [19], which affects the difficulty and process complexity in the device fabrication and/or estimated cost for constructing the structure. Nevertheless, it is ambiguous to quantify the design complexity or topological variation of a certain device structure. To clarify the implications of various PEC device structures on hydrogen production by PEC water splitting, more explicit classification of PEC structures is required.

To develop a systematic structural classification scheme, we first focus on electrical junctions connecting a semiconductor light absorber with surroundings (electrolyte or electrical wire). In the case of the SLJ where the charge carriers directly participate in electrochemical reactions, the reaction is either cathodic or anodic depending on the direction of current flow, and the semiconductor is in contact with an electrolyte with or without a protection layer. Thus, we categorize SLJ into four types: SLJ with cathodic reaction (SLJ-C), SLJ with cathodic reaction and a protection layer (SLJ-PC), SLJ with anodic reaction (SLJ-A) and SLJ with anodic reaction and a protection layer (SLJ-PA). We consider a protection layer if it satisfies the following conditions: the layer is (1) deliberately deposited between a semiconductor and an electrolyte, (2) expected to improve stability of the semiconductor in the PEC environment and (3) thicker than a monolayer thickness. Thus, we do not consider co-catalysts of sub-monolayer thickness, adsorbates or native oxide

Table 1 Classification of electrical junctions on a PV cell in PEC devices

Interface	Classification of electrical junctions
Solid–liquid junction (SLJ)	Cathodic charge transport (SLJ-C)
	Cathodic charge transport across a protection layer (SLJ-PC)
	Anodic charge transport (SLJ-A)
	Anodic charge transport across a protection layer (SLJ-PA)
Solid-state junction (SSJ)	Transparent junction (SSJ-T)
	Opaque junction (SSJ-O)
	Recombination layer (SSJ-R)

Structural classification of a PEC device structure is based on the combination of electrical junctions on semiconductor light absorbers. We classify the electrical junctions into 7 different types, which are cathodic SLJ (SLJ-C), protected cathodic SLJ (SLJ-PC), anodic SLJ (SLJ-A), protected anodic SLJ (SLJ-PA), transparent SSJ (SSJ-T), opaque SSJ (SSJ-O) and a recombination layer (SSJ-R)

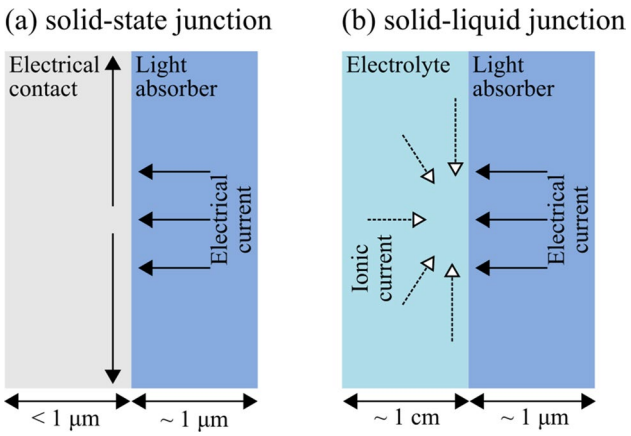

Fig. 1 Electrical junctions on a solid semiconductor. Photo-generated charge carriers can be extracted through either **a** SSJ or **b** SLJ. **a** The extraction through the SSJ requires an electrical current flow along the lateral direction across the large surface of the light absorber. **b** At the SLJ the electrical current through a solid contact is replaced with an ionic current through the electrolyte, which therefore reduces the transport distance to be no more than the thickness of the light absorber. The direction and distance of the ionic current are tunable by the design of a PEC cell

as a protection layer. With regards to the SSJ where the photoexcited charge carriers are extracted to an outer circuit, it is divided as follows: transparent SSJ (SSJ-T), opaque SSJ (SSJ-O). TCO or a patterned metal contact, which is usually deposited on the optical front side of a semiconductor, is a good example of SSJ-T. Meanwhile, SSJ-O is usually applied on the backside where optical transparency is not needed, and it can be constructed by a simple metal layer. In addition, a recombination layer (SSJ-R) is mainly used to monolithically integrate two semiconductors. The 7 different electrical junctions are summarized in Table 1. In this classification scheme, the key difference between SSJ (except SSJ-R) and SLJ is the length of electrical charge transport to drive the PEC reactions. Electrical charges in SSJ-T or SSJ-O have to travel in a lateral direction across a large device surface (see Fig. 1a). On the other hand, the electrical charges in SLJ need to travel only across the thickness of a device, which is typically in the order of a micrometer thickness (see Fig. 1b). The rest of the charge transport is covered by ions in the electrolyte, and the direction and distance of ion transport largely depend on the design of a PEC cell as they travel through the bulk of the electrolyte.

The structure of a PEC device can be classified by the series of electrical junctions placed on semiconductors along the path of an incident light. For example, a photocathode consisting of one semiconductor which has one SLJ with a protection layer on its optical front side and one SSJ on its backside (Fig. 2a) can be described as [SLJ-PC/SSJ-O]. Likewise, wired tandem PEC device and wireless tandem PEC device depicted in Fig. 1b and c can be expressed as [SSJ-T/SLJ-A] [SLJ-PC/SSJ-O] and [SLJ-A/SSJ-R/SLJ-PC], respectively.

As mentioned before, the advantage of PEC over PV + EC lies in (1) an extended surface area reducing the current density and therefore overpotentials, (2) SLJ consuming photo-excited charge carriers on-site without transporting

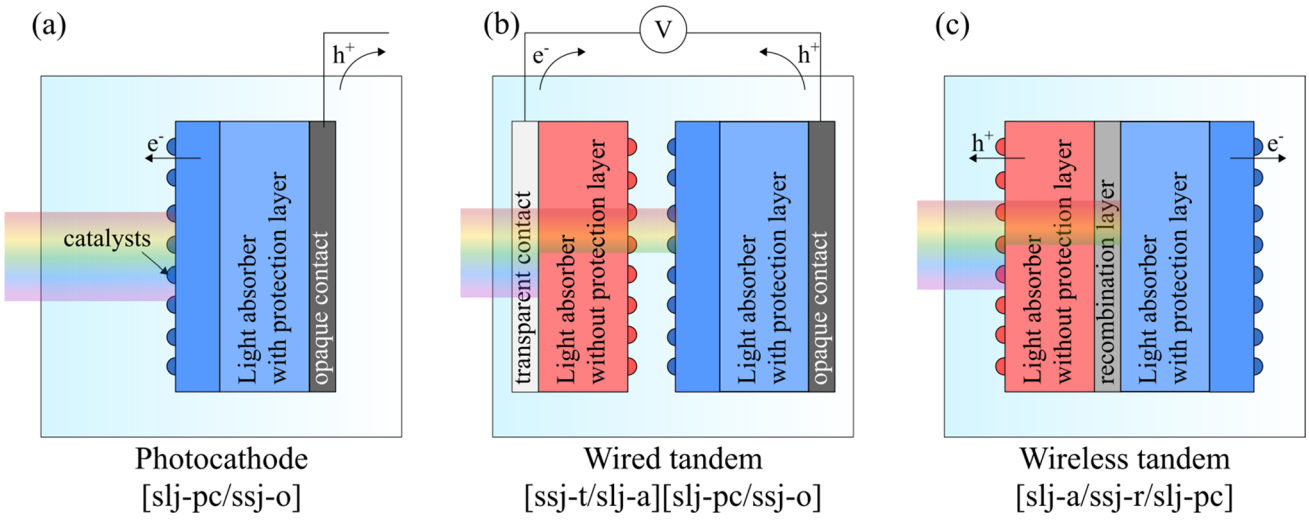

Fig. 2 Schematic drawing of the selected PEC device structures. The classification scheme introduced in this study is explained with the selected PEC device structures as examples. In this classification scheme, **a** photocathode with a protection layer, **b** wired tandem, and **c** wireless tandem devices. In both **b** and **c**, a wider bandgap top cell serves as a photoanode and a lower bandgap bottom cell as a photocathode

across a large area and (3) potential cost reduction from simplifying device structure. While any PEC devices dispersing water-splitting catalysts over the wide surface of the light absorber can take the first advantage, the second advantage—minimization of Ohmic losses from TCO's and power electronics—can be only exploited when losses from ionic transport in a PEC reactor is successfully minimized as well. The ion transport may exhibit ohmic loss from the resistance of electrolyte or pH-gradient loss from local pH variation at the surface of electrodes. There have been studies showing that the losses from the ion transport can be reduced by using a highly acidic (pH 0 or lower) or alkaline (pH 14 or higher) electrolyte [20], designing a PEC reactor with a better ion transport [20–22], and flowing an electrolyte continuously [23] (which is necessary for a practical device operation). In this regard, monolithic wireless PEC devices, such as [SLJ-A/SSJ-R/SLJ-C] or [SLJ-C/SSJ-R/SLJ-A] (analogous to Fig. 1c) would be the most ideal structure because they can dramatically reduce electrical ohmic loss by eliminating the need for a long distance carrier transport over the area of the PEC device. One may dispute that the monolithic wireless structures may pose issues associated with ohmic or pH-gradient loss from ion transport between the cathode and the anode; however, there are early works on PEC devices and reactor designs showing a minimal loss from the electrolyte by using a louvered cell [20] or a perforated cell [21]. Nevertheless, the monolithic wireless configurations have not been extensively investigated, which is most likely due to many complexities and difficulties in the device fabrication and characterization. Most of the reported monolithic wireless tandem devices have been limited to III-V semiconductors or amorphous silicon cells because other light absorbers do not have well-established SSJ-R to integrate them in a tandem configuration. Additionally, characterization of a wireless PEC tandem device is not trivial because it does not have any direct electrical wiring to a potentiostat. Therefore, the performance of the device can be only characterized by collecting gaseous products, which is experimentally more difficult, though more relevant, than collecting electrical charges. We argue that, despite the challenges, the wireless device would be the most ideal PEC structure that can fully exploit the advantages of PEC. Another compromised, yet still attractive, structure is a monolithic PEC device with one SSJ-O wired to a separate EC, such as [SLJ-A/SSJ-R/SSJ-O] or [SLJ-C/SSJ-R/SSJ-O]. Although electrical charges are transported along SSJ-O to EC over a long distance, it is easier to acquire a low sheet resistance at a lower cost compared to SSJ-T.

In PEC devices that include SSJ-T lateral electrical charge transport within a TCO layer results in a severe efficiency loss from ohmic resistance, especially when the device becomes larger for practical solar hydrogen production. A previous theoretical study estimated a voltage loss of ~350 mV from two TCO layers when the lateral dimension of the device was scaled up to ~8 cm (TCO conductivity: 10^5 S/m, TCO thickness: 500 nm, current density: 10 mA/cm^2) [23]. Another theoretical study [24] predicted that enlarging lab-scale (~1 cm^2) PEC devices to a more practical size (~100 cm^2) would lead to 20–30% reduction in the photocurrent (calculation parameters are adapted from other experimental works). A previous experimental study [25] showed confirmed that enlarging a $BiVO_4$ photoanode with SSJ-T from 0.24 to 50 cm^2 reduced the photocurrent by ~65%, but the depletion of ions in the neutral electrolyte also contributed to the efficiency

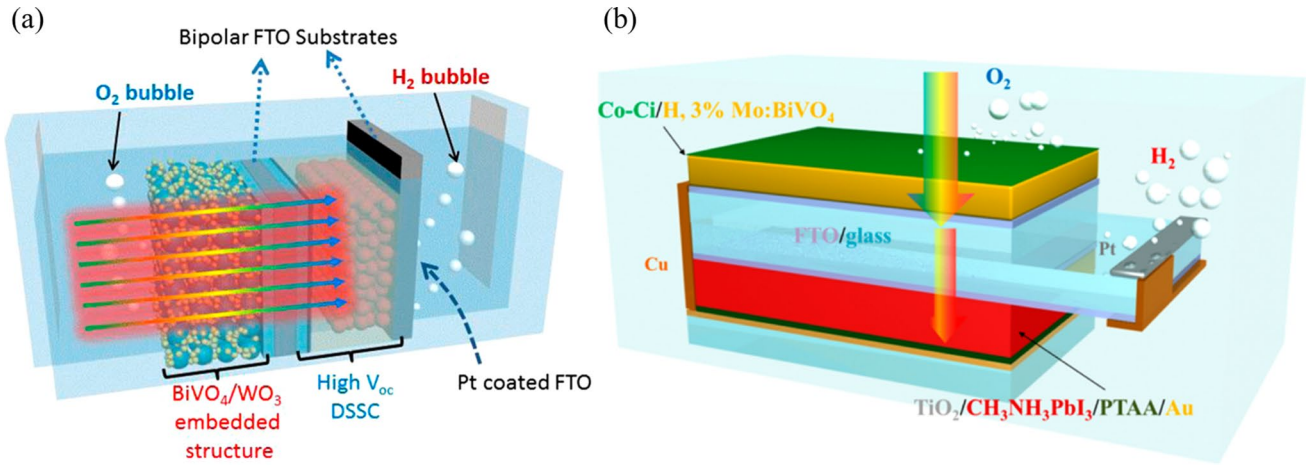

Fig. 3 Examples of PEC device structure classification (adapted from Refs. [26] and [27]). Based on the classification scheme introduced in this study, device structures with SSJ-T are effectively considered as "wired" structures. Some of PEC device structures demonstrated by previous works are effectively "wired" structures, although the structure is seemingly "wireless", because there are **a** three SSJ-T (Reprinted with permission from Ref. [26]. Copyright (2015) Elsevier), and **b** two SSJ-T and one SSJ-O (Reprinted with permission from Ref. [27]. Copyright (2015) American Chemical Society)

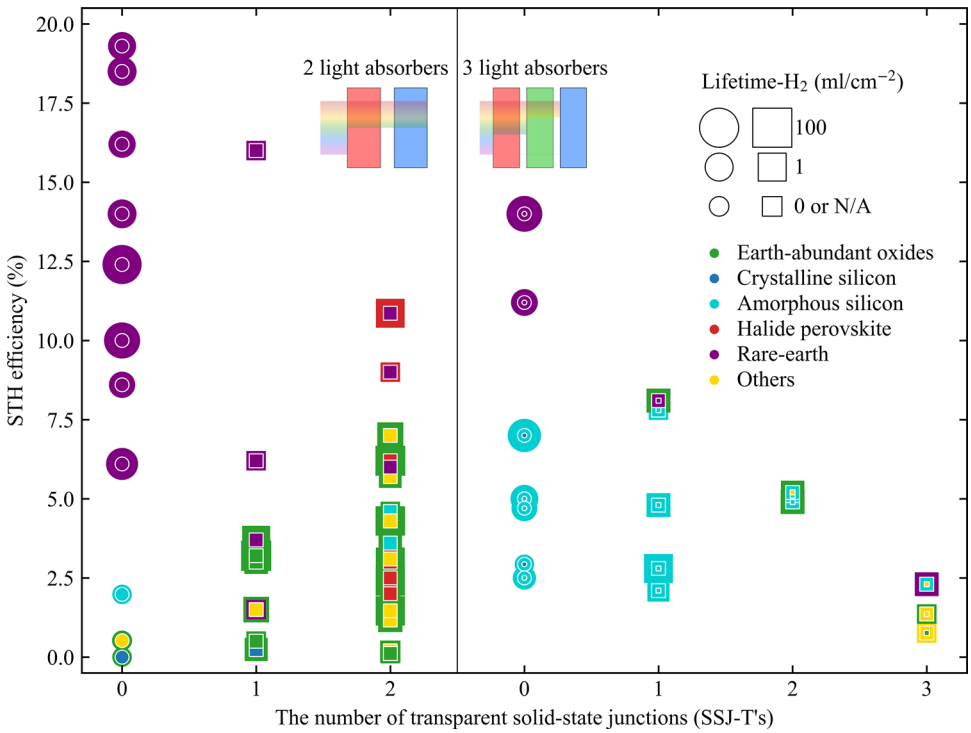

Fig. 4 STH efficiencies from previous studies [7, 8, 11, 21, 26–74] as function of the number of SSJ-T's. The shape of the data points represents the inclusion of SSJ-T in a device structure (circle: not included, rectangle: included). The colors of outer, middle (for devices with three light absorbers) and inner circle or rectangle corresponds to top, middle (for devices three light absorbers) and bottom cell materials, respectively. Different colors represent different light absorbers (green: earth-abundant oxide, blue: crystalline Si, light blue: amorphous Si, red: halide perovskite, purple: any materials containing In, As or Ge, yellow: others, which are mostly chalcogenides and organics). The size of datapoint represents lifetime-H_2 in log scale

loss in this case. We notice that some PEC devices categorized as "wireless" include SSJ-T in their structure as shown in Fig. 3 [26, 27]. In our classification scheme, these structures are effectively "wired" configuration because a similar level of efficiency loss from SSJ-T is expected when the devices are scaled up. To avoid the ohmic loss from the lateral transport, a metal grid can be introduced to SSJ-T [28]; however, introducing the additional patterning process for the metal grid nullifies the advantage of PEC, that is simplified manufacturing process and reduced system cost. Additionally, the metal grid reduces the active area for light absorption.

Despite of these shortcomings from SSJ-T, current research on PEC devices is inclined to the structures with SSJ-T as they are easier to be prepared and tested. Figure 4 presents a collection of previous studies [7, 8, 11, 21, 26–74] on PEC water-splitting devices—solar-to-hydrogen (STH) conversion efficiencies versus the number of SSJ-T's. The shape of data points represents the existence of SSJ-T in a device structure (circle: a structure without SSJ-T, rectangle: a structure

with SSJ-T). The number of concentric circle or square represents the number of light absorbers in a PEC device. More specifically, the outer, middle (for three light absorbers) and inner circle or square corresponds to the top, middle (for three light absorbers) and bottom cell in a PEC device, respectively. The color of each circle or square represents a light absorber material (red: halide perovskite, green: earth-abundant metal oxide, blue: crystalline Si, light blue: amorphous Si, purple: any materials containing rare-earth elements such as In, As or Ge, yellow: others). The light absorber materials marked in purple (rare-earth) are mostly III-V solar cells and some Cu(In, Ga)(S, Se)$_2$, and yellow (others) are mostly earth-abundant chalcogenides or organic solar cells. The size of the datapoints are proportional to the amount of hydrogen produced over the lifetime of a PEC device (lifetime-H_2), and it represents the stability of the device. The lifetime-H_2 value is acquired from gas chronoamperometry (or other gas collection methods) when it is available, or it is estimated from chronoamperometry assuming 100% Faradaic efficiency. It is clear from Fig. 4 that PEC devices based on earth-abundant materials (red, green, blue and yellow) except amorphous silicon (light blue) are more likely to be constructed with SSJ-T than those based on III-V semiconductors with rare elements (purple data points). The preference toward the structures containing SSJ-T must be due to the difficulties in finding a suitable candidate for SSJ-R and monolithically integrating them into a tandem device. For III-V semiconductors, which have been heavily investigated for concentrated PV application, monolithic integration of two or more III-V's via SSJ-R has been well established. On the contrary, the development of SSJ-R's for many earth-abundant metal-oxide materials is still under investigation, and most of the tandem devices based on earth-abundant metal-oxide have relied on coupling separate photoelectrodes using SSJ-T. However, as discussed before, tandem PEC devices employing SSJ-T pose limitations in terms of large scaling and system cost, therefore, we need to steer our efforts towards the wireless construction including SSJ-R to realize PEC water splitting as a means for practical solar hydrogen production.

Another important factor that should be considered for a viable deployment of PEC is the collection and storage of high purity hydrogen at high pressure, and it requires hermetical sealing, gas separation membrane and operation at elevated pressure. In this sense, PEC structures producing hydrogen over a large area may appear less attractive than other structures with a separate hydrogen-producing EC because of difficulties in ensuring reliable sealing [75]. Furthermore, hydrogen produced over a large area with a low current density in a pressurized reactor would increase hydrogen concentration in an oxygen compartment (or vice versa), and it may even reach a hazardous level depending on the PEC reactor design [76, 77]. Therefore, a monolithic photoanode which can separate a hydrogen-producing counter electrode, for example [SLJ-A/SSJ-R/SSJ-O], can potentially be more beneficial compared to the other structures producing hydrogen over a large area. Separating hydrogen-producing EC by using SSJ-O provides flexibility in the reactor design, at the cost of the Ohmic loss from the charge transport over a long distance, and it may facilitate sealing the PEC cell hermetically. Moreover, some previous studies introduced redox mediators to isolate HER from PEC reactor to avoid any possibility of the product crossover [78, 79].

3 Semiconductor light absorber materials

As well as the device structure, the choice of a light absorber material is one of the most critical factors affecting various aspects of device performance such as STH efficiency, stability and scalability of a PEC device. The theoretical maximum of STH efficiency is determined by the band gaps of the light absorber materials. Previous theoretical studies [80, 81] have shown that, in the cases of PEC devices consisting of two light absorbers, the optimal combination of the band gaps are ~1.8 eV and ~1.1 eV, respectively, in view of Shockley-Queisser limit, electrocatalytic overpotentials and the light absorption by water. However, actual STH efficiencies tend to be lower than the theoretical expectations because of a charge collection efficiency that is less than unity and other parasitic losses. Concerning the overall stability of a PEC device, the electrochemical stability of the materials is the main concern because they are in direct contact with (or in close vicinity of) electrolytes at SLJ. Light absorbers with poor electrochemical stability may limit the operational range of pH's of electrolyte or alternatively force the structures with SSJ rather than SLJ to be employed. Along with the electrochemical stability, the stability in air or device fabrication environments also needs attention. Regarding the scalability, we discussed that ohmic loss would limit the practical size of a PEC device to several centimeters. Another consideration on the scalability issue is the natural abundance of materials. When considering world energy consumption [82], an energy conversion device should be scalable to TW-scale. Building PEC devices capable of producing fuels in terawatt-scale would require several hundreds kilo-tons/TW of light absorber materials [83], and therefore, materials with enough global supply are of greater interest. To maximize these performance parameters (STH efficiency, stability

and scalability), all semiconductor materials constituting each cell and device should be taken into account simultaneously. In the following sections, we will survey combinations of materials together with compatible device structures used for constructing PEC devices and assess them in terms of STH efficiency, stability and scalability, and a broad outline of the survey is summarized in Table 2.

3.1 Earth-abundant top cell/crystalline silicon

Although single crystalline silicon has poor light absorbance and requires an energy-intensive ingot growth process, it has gained popularity and dominance in the PV market over other competing technologies because of its wide availability [84]. The bandgap of silicon is 1.12 eV, which is an ideal value as a bottom cell for a double-junction tandem PEC device. In coupling with a silicon bottom cell, various earth-abundant metal oxides have been investigated as a top cell to retain the scalability of tandem devices in TW scale [58, 64, 68, 85]. Metal oxides with various compositions providing opportunities for tuning bandgap and optoelectronic properties have been widely studied [86], however, most metal oxides have sluggish carrier transport properties because of strong electron–phonon interaction originating from the highly ionic bonding nature [87–89]. In addition, a carrier lifetime tends to be shorter than other PV materials due to fast recombination at bulk defects or surface states [89]. As such, metal oxides in general produce much smaller photovoltage and photocurrent compared to maximum theoretically predicted values. Thus, recent metal oxide photoelectrode studies focus on improving charge transfer kinetics by various strategies: (1) introducing an internal electric field via forming heterojunction to facilitate electron–hole separation [90], (2) adding dopants to enhance bulk conductivity and reduce bulk recombination [91, 92], and (3) nanostructuring surface to facilitate charge collection [93]. As of now, unassisted solar water splitting by a tandem device based on metal oxide and crystalline silicon has been rarely demonstrated yet [58, 64, 68, 85] because photovoltage and photocurrent from the metal oxide top cell are still much lower than the theoretical limits. Among earth-abundant candidates for a top cell in tandem PEC cells with a silicon bottom cell, $BiVO_4$ has been the most successful material thanks to better carrier transporting properties than other metal oxides and its large band gap (2.4 eV) that allows a high photovoltage. Several $BiVO_4$/crystalline Si studies have reported unassisted solar water splitting but the reported STH efficiencies remain in the range of 0–1% [58, 64]. There have been attempts to increase a photovoltage from a bottom cell by replacing the crystalline silicon with other earth-abundant light absorbers with a larger bandgap; however, the larger photovoltage is accompanied by the reduced photocurrent, resulting in the loss of STH efficiency. Considering the ideal combination of the band gaps, one may find metal chalcogenides or metal halides with superior optoelectronic properties as an attractive candidate for the top cell instead of metal oxides. For example, a dry tandem solar cell consisting of a metal halide perovskite and crystalline silicon has made rapid progress in recent years, achieving the power conversion efficiency of 29% [94] and this could be applied to PEC energy conversion with proper protection against a liquid electrolyte. Perovskite/crystalline Si does not contain rare-earth elements and it has already demonstrated exceptionally high power conversion efficiency, and therefore it has merits in STH efficiency and TW scalability.

However, for any PEC device that makes a junction between a light absorber and an electrolyte, the electrochemical stability of the materials is a prime concern. Light absorbers that are stable in a highly acidic or alkaline electrolyte are preferred because it would be much easier to design a PEC cell with a low pH gradient and ohmic losses from ion transport. One of the main reasons behind the popularity of Fe_2O_3 photoanode is its stability in alkaline electrolytes. On the other hand, $BiVO_4$ is stable only in a near-neutral range (pH 4–10), and scaling up $BiVO_4$ PEC device would pose a significant challenge in designing a PEC reactor due to high electrical resistance of the electrolyte. Figure 5 shows STH efficiencies reported from previous studies depending on pH's of electrolytes and device configuration (PV + PEC configuration represents a wire-connection between a PEC device with SLJ and conventional PV-like device.). As can be confirmed from Fig. 5a and b, metal oxide materials (green) are mostly tested in the near-neutral pH range because of the stability issue. For the operation in a highly acidic or alkaline electrolyte, a protection layer should be deposited over the surface of a light absorber to avoid direct contact with the electrolyte. Protecting SLJ for the operation under dark can be easily achieved by depositing a thick and dense layer on a clean surface [74] or attaching a metal substrate [95] (shown in Fig. 5c). For illumination conditions, SLJ is usually protected by a large bandgap oxide thin film. Depending on the electrochemical reaction on its surface, the oxide layer should be either n-type or p-type for transporting electrons or holes, respectively. TiO_2 has been widely used as an electron transporting protection layer due to its transparency and stability over a broad range of pH's [96]. Interestingly, TiO_2 turns out to be compatible with either n-type or buried p–n junction silicon photoanode [97–100] although TiO_2 is intrinsically n-type oxide. To protect a photoanode in alkaline

Table 2 Summary of light absorber materials in terms of STH efficiency, stability, and scalability

Light absorber materials	STH efficiency	Stability in acidic or alkaline electrolytes	Scalability to TW scale
Earth-abundant top cell/crystalline silicon	Low Most research efforts are focused on developing efficient top cells	Low There are only a few top cell materials stable in extreme pHs (e.g., WO_3 in acid, Fe_2O_3 in alkaline)	High However, most of the devices are tested with SSJ-T, and it limits extending device area to cm-scale
Epitaxial III-V thin films	High The best STH efficiencies have been achieved with III-V light absorbers	Low Most of the III-V materials are unstable at extreme pHs	Low The supply of In, As and Ge is severely limited

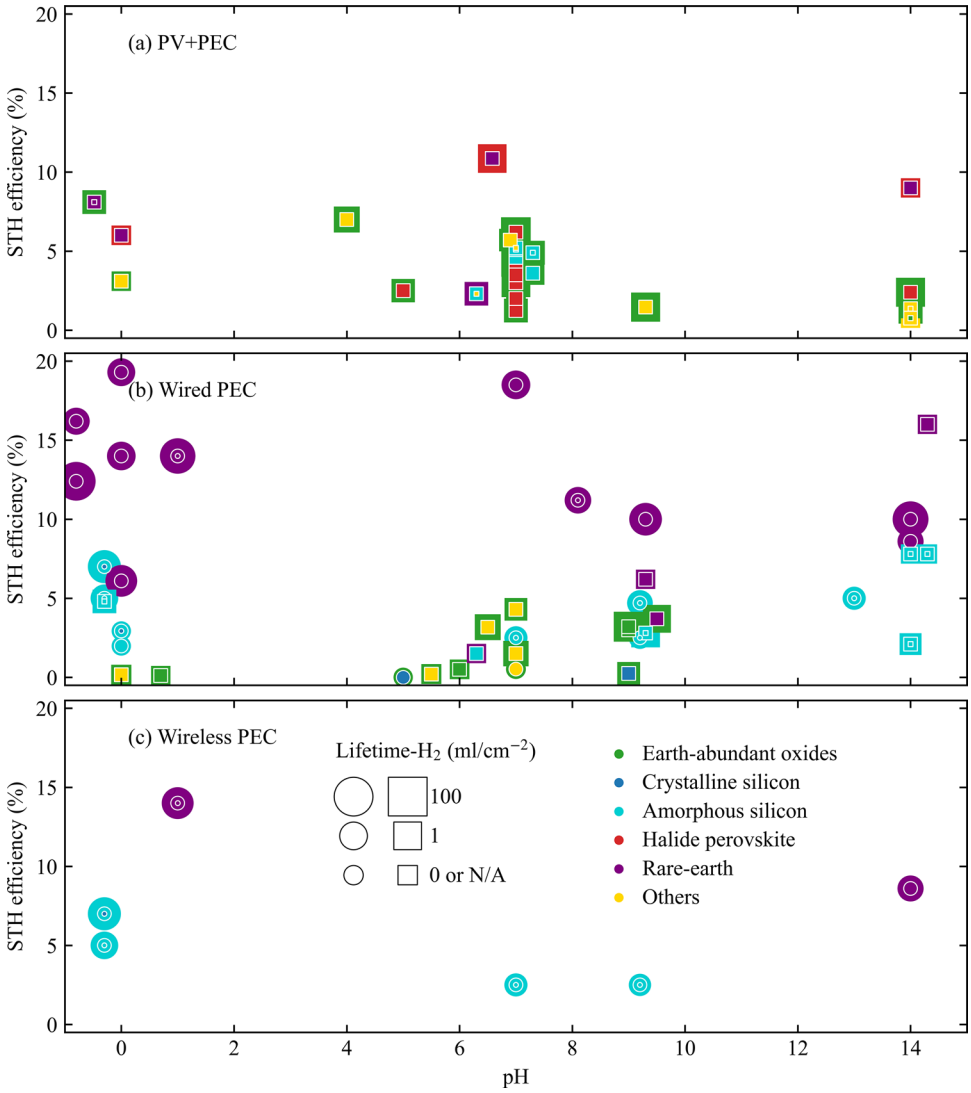

Fig. 5 STH efficiency from the previous studies [7, 8, 11, 21, 26–74] depending on the pH of the electrolyte and the device structures: **a** PV + PEC, **b** Wired PEC and **c** Wireless PEC. The shape of the data points represents the inclusion of SSJ-T in a device structure (circle: not included, rectangle: included). The colors of outer, middle (for devices with three light absorbers) and inner circle or rectangle corresponds to top, middle (for devices three light absorbers) and bottom cell materials, respectively. Different colors represent different light absorbers (green: earth-abundant oxide, blue: crystalline Si, light blue: amorphous Si, red: halide perovskite, purple: any materials containing In, As or Ge, yellow: others, which are mostly chalcogenides and organics). The size of datapoint represents lifetime-H_2 in log scale

electrolytes, p-type NiO is an attractive option as it is a large bandgap (~3.6 eV) p-type semiconductor [101]. Besides, NiO can also serve as a good OER catalyst in alkaline electrolytes. Other noble metal oxide protection layers such as CoO_x, SnO_2 and Nb_2O_5 are noteworthy [96], and introducing a proper protection layer would broaden the scope of available light absorber materials for PEC application. However, the most critical issue in the protection layer is ensuring a complete impermeability over the entire surface area of a light absorber. For example, small foreign particles sitting on a surface may introduce pin holes in the protection layer, and the presence of a single pinhole would lead to the corrosion of the entire light absorber underneath the protection layer.

The challenge in the impermeability becomes clear when it comes to metal halide perovskites, which are discussed as an attractive top cell material in terms of STH efficiency and TW scalability. The metal halide perovskites are very unstable when in contact with oxygen, and the degradation is accelerated in the presence of water molecules. Thus, depositing an impermeable protection layer is vital for applying SLJ on a halide perovskite absorber, which is not a trivial task. As shown in Fig. 5a, most previous studies with a halide perovskite are tested in PV + PEC configuration [27, 32, 34–36, 40, 57, 69–71], which encapsulates the halide perovskite by using SSJ-T like a conventional PV. There is a previous work [102] on improving the impermeability of TiO_2 protection layer on a halide perovskite photocathode by atomic layer deposition, and it demonstrated around 2 h of lifetime. With such an effort to improve the impermeability, the very appealing optoelectronic properties of halide perovskite materials could be utilized without the losses from SSJ-T.

With regards to the stability of silicon bottom cell, it can benefit from the previous studies on transparent protection layers for silicon photoelectrodes [9, 14, 15, 97–100, 103–106]. The silicon photoelectrodes in acidic electrolytes are mostly stable even with an imperfect protection layer by forming a native oxide layer between the protection layer and silicon, but less stable in alkaline electrolytes [98]. In cases of monolithic devices, however, transparent SLJ is not necessary for silicon (or any other) bottom cell because an electrochemical reaction always takes place at a dark side while the optical front side is covered with a top cell.

3.2 Epitaxial III-V thin films

III-V semiconductor light absorbers epitaxially grown on a seed wafer possesses outstanding optoelectronic properties and solar cells based on these materials have achieved record-high power conversion efficiencies [107]. Moreover, tandem devices based on III-V light absorbers have well-established processes for recombination layers. Accordingly, PEC devices comprising III-V semiconductors demonstrated the highest STH efficiencies as shown in Figs. 4, 5 and 6 [8, 38, 44–46, 49, 51, 59–63, 74]. Structures without SSJ-T would be preferred because they can avoid using a complicated combination of materials often required to place a metal grid contact on a III-V light absorber. Thus, a wireless monolithic structure or monolithic structure with one SSJ-O has been a popular choice for III-V based tandem PEC devices as shown in Fig. 5b and c. However, scalability in TW scale would be severely limited due to the scarcity of indium and gallium. Hence, there have been efforts to minimize the loading of III-V materials in PEC devices by taking similar approaches used for III-V solar cells [108]. Because most of the incidence of light can be absorbed by a III-V film of only several hundred-nanometer thicknesses, a single crystal seed wafer with hundred-micrometer thickness is not an integral part of a PEC device. Therefore, exfoliation and transfer of a III-V thin film to another substrate allows the possibility of reusing the seed wafer for another epitaxial growth, which can reduce the consumption of expensive III-V materials [62]. Another approach to improve electricity production per raw material usage is the use of concentrating incoming light on a small PEC device [59, 109]. A concentrated PEC reactor would be operating with a high current density possible at an elevated temperature and therefore requires significant efforts for balancing many factors (thermodynamic voltage, charge carrier recombination, ohmic losses from components), which will result in both beneficial and adverse effects. In addition, it should be noted that the concentrated PEC reactor may utilize waste heat from a reactor while cycling an electrolyte [109].

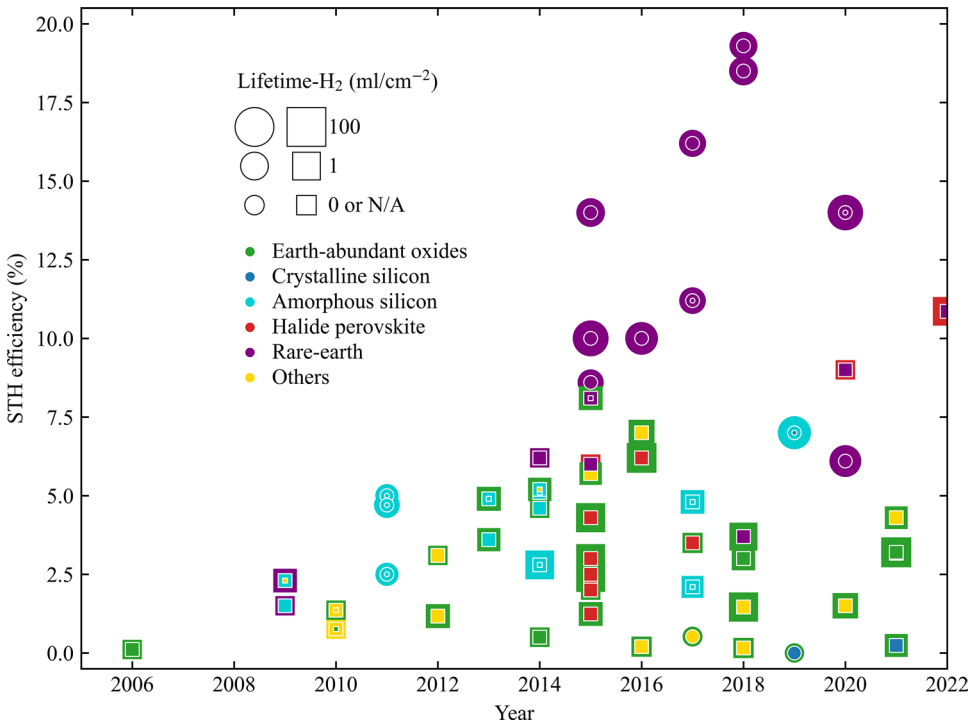

Fig. 6 STH efficiency from the previous studies [7, 8, 11, 21, 26–74] over the years. The shape of the data points represents the inclusion of SSJ-T in a device structure (circle: not included, rectangle: included). The colors of outer, middle (for devices with three light absorbers) and inner circle or rectangle corresponds to top, middle (for devices three light absorbers) and bottom cell materials, respectively. Different colors represent different light absorbers (green: earth-abundant oxide, blue: crystalline Si, light blue: amorphous Si, red: halide perovskite, purple: any materials containing In, As or Ge, yellow: others, which are mostly chalcogenides and organics). The size of datapoint represents lifetime-H_2 in log scale

Another challenge that needs to be overcome is the stability of III-V materials in electrochemical environments because most III-V materials are stable only in the near-neutral pH. Similar to the metal oxides or silicon, protection layers can be applied to III-V to avoid a direct contact with an electrolyte. III-V light absorbers have a better chance to improve the impermeability of a protection layer by growing a protection layer epitaxially in the same growth chamber without exposing them to atmosphere. For example, a GaInP protection layer with only 10 nm thickness improves the stability of a PEC device significantly [62], although the stability of GaInP in acid may not be good enough for long-term operation for a practical application.

4 Conclusion and outlook

According to the techno-economic analyses [110–112], a significant level of development is necessary to realize a practical solar hydrogen production by PEC. The analyses show that current PEC devices need significant improvement, especially in stability, while keeping the system cost as low as possible. The most limiting factor in stability of a PEC device is the electrochemical stability of light absorber materials, and the system cost would be heavily dependent on a PEC device structure. Therefore, in this review, we introduce the pressing/potential issues in PEC within the framework of device structures and light absorber materials. We address that our research efforts should be focused on (1) the optimization of a PEC reactor design for electrical/ionic charge transport and (2) a reliable collection of H_2 product. It is also essential to develop an efficient, stable and scalable large bandgap (~ 1.8 eV) light absorber materials. There have been two different approaches to light absorber development, which are (3) improving the efficiency of earth-abundant light absorber materials and developing SSJ-R for monolithic integration, or (4) overcoming the TW-scalability issue of rare-earth light absorbers. (5) Besides, both types of materials require a significant improvement in stability.

Electrical/ionic charge transport through a PEC device and reactor should be finely optimized and result in lower losses compared to that in PV + EC. We suggested a classification scheme for PEC device structure that can clarify the electron/ion transport characteristics of a PEC device, and argued that device structures without SSJ-T can minimize the loss from electrical charge transport over a long distance. Optimization of ion transport in PEC reactor is in the early stage of development, and the losses from the ion transport can be minimized by circulating an electrolyte with an extreme pH with a high flow rate and developing a novel PEC reactor design.

The collection of hydrogen should not be overlooked, especially when using a device structure producing hydrogen over a large surface of a light absorber at elevated pressure. Although it is not straightforward to estimate costs for hermetic sealing over a large area and figure out the gas product crossover through a membrane in a pressurized PEC cell in this stage, the structures with a separate hydrogen-producing EC might be attractive for the facile collection of hydrogen.

Silicon is an ideal light absorber material for a bottom cell, however, suitable light absorber materials for a top cell that can be monolithically integrated on silicon have not been developed yet. We categorize the light absorber materials based on crustal abundance (earth-abundant/rare-earth), which is the main factor that determines the scalability in TW-scale, and each category of materials has different issues. Earth-abundant materials would be scalable to TW-scale, however, they show much lower STH efficiencies than the rare-earth materials because of poor optoelectronic properties. In addition, tandem devices based on earth-abundant materials are mostly tested with a device structure with SSJ-T due to the lack of recombination layer, but it may limit the scaling up of the PEC device to larger than cm-scale because of the electrical losses from SSJ-T.

On the other hand, previous studies based on rare-earth materials show superior STH efficiency in monolithic device structures, but they rely on scarce elements such as In, As and Ge. Therefore, efforts should be directed to the epitaxial thin film transfer or concentrated PEC in order to overcome the poor TW-scalability. In addition, concentrated PEC may provide the chance to utilize waste heat from a PEC reactor so that it can further enhance its economic feasibility.

We also emphasized that the stability of PEC devices is not satisfactory yet for practical solar hydrogen production. Ben-Naim et al. [38] proposed the concept of lifetime-H_2 and claimed that lifetime-H_2 should be larger than ~ 100 L/cm^2 to acquire economic feasibility. However, the state-of-art PEC devices generate around ~ 0.1 L/cm^2 over their lifetime as shown in Fig. 7, and there is still around three orders of magnitude discrepancy between the goal and the current

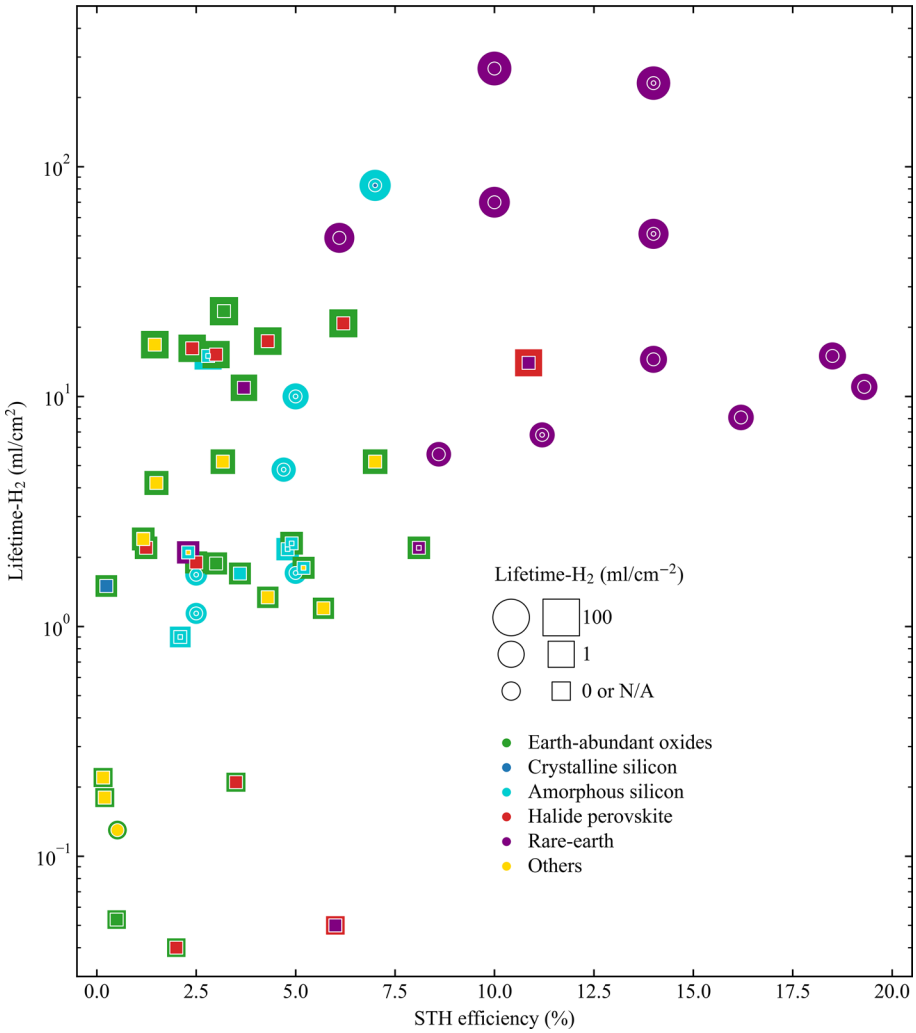

Fig. 7 STH efficiency and lifetime-H_2 from the previous studies [7, 8, 11, 21, 26–74]. The shape of the data points represents the inclusion of SSJ-T in a device structure (circle: not included, rectangle: included). The colors of outer, middle (for devices with three light absorbers) and inner circle or rectangle corresponds to top, middle (for devices three light absorbers) and bottom cell materials, respectively. Different colors represent different light absorbers (green: earth-abundant oxide, blue: crystalline Si, light blue: amorphous Si, red: halide perovskite, purple: any materials containing In, As or Ge, yellow: others, which are mostly chalcogenides and organics). The size of datapoint represents lifetime-H_2 in log scale

level. The stability of a PEC device would be enhanced by ensuring the complete impermeability to avoid direct contact between a light absorber material and an electrolyte.

Acknowledgements This work was supported by a National Research Foundation of Korea (NRF) grant funded by the Korean government. (No. 2021M3I3A1085009). This research was supported by the Nano Material Technology Development Program (Green Nano Technology Development Program) through the NRF funded by the Ministry of Education, Science and Technology (No. 2018M3A7B4065662).

Author contributions Both the authors contributed to the conceptualization. Literature search and analysis were performed by CM. The first draft of the manuscript was written by CM and all authors commented on previous versions of the manuscript. Both the authors read and approved the final manuscript.

Funding This work was supported by a National Research Foundation of Korea (NRF) Grant funded by the Korean government. (No. 2021M3I3A1085009). This research was supported by the Nano Material Technology Development Program (Green Nano Technology Development Program) through the NRF funded by the Ministry of Education, Science and Technology (No. 2018M3A7B4065662).

Data availability Not applicable.

Code availability Not applicable.

Declarations

Competing interests The authors declare that there is no competing interests.

References

1. UNFCCC. Kyoto protocol. Rio de Janeiro: UNFCCC; 1997.
2. UNFCCC. Paris agreement. Rio de Janeiro: UNFCCC; 2015.
3. The Future of Hydrogen. The future of hydrogen. OECD. 2019. https://doi.org/10.1787/1e0514c4-en.
4. van de Krol R, Parkinson BA. Perspectives on the photoelectrochemical storage of solar energy. MRS Energy Sustain. 2017;4:13. https://doi.org/10.1557/mre.2017.15.
5. Choi J, Song JT, Jang HS, Choi M-J, Sim DM, Yim S, et al. Interfacial band-edge engineered TiO_2 protection layer on Cu_2O photocathodes for efficient water reduction reaction. Electron Mater Lett. 2017;13:57–65. https://doi.org/10.1007/s13391-017-6316-1.
6. Ji L, McDaniel MD, Wang S, Posadas AB, Li X, Huang H, et al. A silicon-based photocathode for water reduction with an epitaxial $SrTiO_3$ protection layer and a nanostructured catalyst. Nat Nanotechnol. 2015;10:84–90. https://doi.org/10.1038/nnano.2014.277.
7. Yang W, Kim JH, Hutter OS, Phillips LJ, Tan J, Park J, et al. Benchmark performance of low-cost Sb_2Se_3 photocathodes for unassisted solar overall water splitting. Nat Commun. 2020;11:861. https://doi.org/10.1038/s41467-020-14704-3.
8. Kobayashi H, Sato N, Orita M, Kuang Y, Kaneko H, Minegishi T, et al. Development of highly efficient $CuIn_{0.5}Ga_{0.5}Se_2$-based photocathode and application to overall solar driven water splitting. Energy Environ Sci. 2018;11:3003–9. https://doi.org/10.1039/C8EE01783B.
9. Ros C, Andreu T, Hernández-Alonso MD, Penelas-Pérez G, Arbiol J, Morante JR. Charge transfer characterization of ALD-grown TiO_2 protective layers in silicon photocathodes. ACS Appl Mater Interfaces. 2017;9:17932–41. https://doi.org/10.1021/acsami.7b02996.
10. Trześniewski BJ, Smith WA. Photocharged $BiVO_4$ photoanodes for improved solar water splitting. J Mater Chem A. 2016;4:2919–26. https://doi.org/10.1039/C5TA04716A.
11. Han L, Abdi FF, van de Krol R, Liu R, Huang Z, Lewerenz H-J, et al. Efficient water-splitting device based on a bismuth vanadate photoanode and thin-film silicon solar cells. Chemsuschem. 2014;7:2832–8. https://doi.org/10.1002/cssc.201402456.
12. Byun S, Jung G, Moon S-Y, Kim B, Park JY, Jeon S, et al. Compositional engineering of solution-processed $BiVO_4$ photoanodes toward highly efficient photoelectrochemical water oxidation. Nano Energy. 2018;43:244–52. https://doi.org/10.1016/j.nanoen.2017.11.034.
13. Noh K-J, Kim B-R, Yoon G-J, Jung S-C, Kang W, Kim S-J. Microstructural effect on the photoelectrochemical performance of hematite-Fe_2O_3 photoanode for water splitting. Electron Mater Lett. 2012;8:345–50. https://doi.org/10.1007/s13391-012-2007-0.
14. Chuang C-H, Lai Y-Y, Hou C-H, Cheng Y-J. Annealed polycrystalline TiO_2 interlayer of the n-Si/TiO_2/Ni photoanode for efficient photoelectrochemical water splitting. ACS Appl Energy Mater. 2020;3:3902–8. https://doi.org/10.1021/acsaem.0c00319.
15. Scheuermann AG, Lawrence JP, Kemp KW, Ito T, Walsh A, Chidsey CED, et al. Design principles for maximizing photovoltage in metal-oxide-protected water-splitting photoanodes. Nat Mater. 2016;15:99–105. https://doi.org/10.1038/nmat4451.
16. Zhang K, Ma M, Li P, Wang DH, Park JH. Water splitting progress in tandem devices: moving photolysis beyond electrolysis. Adv Energy Mater. 2016;6:1–16. https://doi.org/10.1002/aenm.201600602.
17. Kim JH, Hansora D, Sharma P, Jang JW, Lee JS. Toward practical solar hydrogen production-an artificial photosynthetic leaf-to-farm challenge. Chem Soc Rev. 2019;48:1908–71. https://doi.org/10.1039/c8cs00699g.
18. Sathre R, Greenblatt JB, Walczak K, Sharp ID, Stevens JC, Ager JW, et al. Opportunities to improve the net energy performance of photoelectrochemical water-splitting technology. Energy Environ Sci. 2016;9:803–19. https://doi.org/10.1039/c5ee03040d.
19. Jacobsson TJ, Fjällström V, Edoff M, Edvinsson T. Sustainable solar hydrogen production: from photoelectrochemical cells to PV-electrolyzers and back again. Energy Environ Sci. 2014;7:2056–70. https://doi.org/10.1039/c4ee00754a.
20. Walczak K, Chen Y, Karp C, Beeman JW, Shaner M, Spurgeon J, et al. Modeling, simulation, and fabrication of a fully integrated, acidstable, scalable solar-driven water-splitting system. Chemsuschem. 2015;8:544–51. https://doi.org/10.1002/cssc.201402896.
21. Vijselaar WJC, Perez-Rodriguez P, Westerik PJ, Tiggelaar RM, Smets AHM, Gardeniers H, et al. A stand-alone si-based porous photoelectrochemical cell. Adv Energy Mater. 2019. https://doi.org/10.1002/aenm.201803548.
22. Bedoya-Lora FE, Hankin A, Kelsall GH. En route to a unified model for photoelectrochemical reactor optimization. II–Geometric optimization of perforated photoelectrodes. Front Chem Eng. 2021;3:1–16. https://doi.org/10.3389/fceng.2021.749058.
23. Abdi FF, Gutierrez Perez RR, Haussener S. Mitigating voltage losses in photoelectrochemical cell scale-up. Sustain Energy Fuels. 2020;4:2734–40. https://doi.org/10.1039/d0se00246a.
24. Holmes-Gentle I, Agarwal H, Alhersh F, Hellgardt K. Assessing the scalability of low conductivity substrates for photo-electrodes via modelling of resistive losses. Phys Chem Chem Phys. 2018;20:12422–9. https://doi.org/10.1039/C8CP01337C.
25. Ahmet IY, Ma Y, Jang J-W, Henschel T, Stannowski B, Lopes T, et al. Demonstration of a 50 cm^2 $BiVO_4$ tandem photoelectrochemical-photovoltaic water splitting device. Sustain Energy Fuels. 2019;3:2366–79. https://doi.org/10.1039/C9SE00246D.
26. Shi X, Zhang K, Shin K, Ma M, Kwon J, Choi IT, et al. Unassisted photoelectrochemical water splitting beyond 5.7% solar-to-hydrogen conversion efficiency by a wireless monolithic photoanode/dye-sensitised solar cell tandem device. Nano Energy. 2015;13:182–91. https://doi.org/10.1016/j.nanoen.2015.02.018.
27. Kim JH, Jo Y, Kim JH, Jang JW, Kang HJ, Lee YH, et al. Wireless solar water splitting device with robust cobalt-catalyzed, dual-doped $BiVO_4$ photoanode and perovskite solar cell in tandem: a dual absorber artificial leaf. ACS Nano. 2015;9:11820–9. https://doi.org/10.1021/acsnano.5b03859.

28. Becker J-P, Turan B, Smirnov V, Welter K, Urbain F, Wolff J, et al. A modular device for large area integrated photoelectrochemical water-splitting as a versatile tool to evaluate photoabsorbers and catalysts. J Mater Chem A. 2017;5:4818–26. https://doi.org/10.1039/C6TA10688A.
29. Rocheleau RE, Miller EL, Misra A. High-efficiency photoelectrochemical hydrogen production using multijunction amorphous silicon photoelectrodes. Energy Fuels. 1998;12:3–10. https://doi.org/10.1021/ef9701347.
30. Zhang Y, Lv H, Zhang Z, Wang L, Wu X, Xu H. Stable unbiased photo-electrochemical overall water splitting exceeding 3% efficiency via covalent triazine framework/metal oxide hybrid photoelectrodes. Adv Mater. 2021;33:2008264. https://doi.org/10.1002/adma.202008264.
31. Ye S, Shi W, Liu Y, Li D, Yin H, Chi H, et al. Unassisted photoelectrochemical cell with multimediator modulation for solar water splitting exceeding 4% solar-to-hydrogen efficiency. J Am Chem Soc. 2021;143:12499–508. https://doi.org/10.1021/jacs.1c00802.
32. Baek JH, Kim BJ, Han GS, Hwang SW, Kim DR, Cho IS, et al. $BiVO_4/WO_3/SnO_2$ double-heterojunction photoanode with enhanced charge separation and visible-transparency for bias-free solar water-splitting with a perovskite solar cell. ACS Appl Mater Interfaces. 2017;9:1479–87. https://doi.org/10.1021/acsami.6b12782.
33. Sakai Y, Sugahara S, Matsumura M, Nakato Y, Tsubomura H. Photoelectrochemical water splitting by tandem type and heterojunction amorphous silicon electrodes. Can J Chem. 1988;66:1853–6. https://doi.org/10.1139/v88-299.
34. Qiu Y, Liu W, Chen W, Chen W, Zhou G, Hsu P-C, et al. Efficient solar-driven water splitting by nanocone $BiVO_4$-perovskite tandem cells. Sci Adv. 2016. https://doi.org/10.1126/sciadv.1501764.
35. Zhang X, Zhang B, Cao K, Brillet J, Chen J, Wang M, et al. A perovskite solar cell-TiO_2@$BiVO_4$ photoelectrochemical system for direct solar water splitting. J Mater Chem A. 2015;3:21630–6. https://doi.org/10.1039/C5TA05838D.
36. Dias P, Schreier M, Tilley SD, Luo J, Azevedo J, Andrade L, et al. Transparent cuprous oxide photocathode enabling a stacked tandem cell for unbiased water splitting. Adv Energy Mater. 2015;5:1501537. https://doi.org/10.1002/aenm.201501537.
37. Bornoz P, Abdi FF, Tilley SD, Dam B, van de Krol R, Graetzel M, et al. A bismuth vanadate-cuprous oxide tandem cell for overall solar water splitting. J Phys Chem C. 2014;118:16959–66. https://doi.org/10.1021/jp500441h.
38. Ben-Naim M, Britto RJ, Aldridge CW, Mow R, Steiner MA, Nielander AC, et al. Addressing the stability gap in photoelectrochemistry: molybdenum disulfide protective catalysts for tandem III-V unassisted solar water splitting. ACS Energy Lett. 2020;5:2631–40. https://doi.org/10.1021/acsenergylett.0c01132.
39. Jiang F, Li S, Ozaki C, Harada T, Ikeda S. Co-electrodeposited Cu_2ZnSnS_4 thin film solar cell and Cu_2ZnSnS_4 solar cell—$BiVO_4$ tandem device for unbiased solar water splitting. Sol RRL. 2018;2:1700205. https://doi.org/10.1002/solr.201700205.
40. Chen Y-S, Manser JS, Kamat PV. All solution-processed lead halide perovskite-$BiVO_4$ tandem assembly for photolytic solar fuels production. J Am Chem Soc. 2015;137:974–81. https://doi.org/10.1021/ja511739y.
41. Huang D, Wang K, Li L, Feng K, An N, Ikeda S, et al. 3.17% efficient Cu_2ZnSnS_4–$BiVO_4$ integrated tandem cell for standalone overall solar water splitting. Energy Environ Sci. 2021;14:1480–9. https://doi.org/10.1039/D0EE03892J.
42. Pihosh Y, Turkevych I, Mawatari K, Uemura J, Kazoe Y, Kosar S, et al. Photocatalytic generation of hydrogen by core-shell $WO_3/BiVO_4$ nanorods with ultimate water splitting efficiency. Sci Rep. 2015;5:11141. https://doi.org/10.1038/srep11141.
43. Pan L, Kim JH, Mayer MT, Son M-K, Ummadisingu A, Lee JS, et al. Boosting the performance of Cu_2O photocathodes for unassisted solar water splitting devices. Nat Catal. 2018;1:412–20. https://doi.org/10.1038/s41929-018-0077-6.
44. May MM, Lewerenz H-J, Lackner D, Dimroth F, Hannappel T. Efficient direct solar-to-hydrogen conversion by in situ interface transformation of a tandem structure. Nat Commun. 2015;6:8286. https://doi.org/10.1038/ncomms9286.
45. Okamoto S, Deguchi M, Yotsuhashi S. Modulated III-V triple-junction solar cell wireless device for efficient water splitting. J Phys Chem C. 2017;121:1393–8. https://doi.org/10.1021/acs.jpcc.6b07991.
46. Modestino MA, Walczak KA, Berger A, Evans CM, Haussener S, Koval C, et al. Robust production of purified H_2 in a stable, self-regulating, and continuously operating solar fuel generator. Energy Environ Sci. 2014;7:297–301. https://doi.org/10.1039/C3EE43214A.
47. Wang X, Peng K-Q, Hu Y, Zhang F-Q, Hu B, Li L, et al. Silicon/hematite core/shell nanowire array decorated with gold nanoparticles for unbiased solar water oxidation. Nano Lett. 2014;14:18–23. https://doi.org/10.1021/nl402205f.
48. Shao D, Zheng L, Feng D, He J, Zhang R, Liu H, et al. TiO_2–P_3HT:PCBM photoelectrochemical tandem cells for solar-driven overall water splitting. J Mater Chem A. 2018;6:4032–9. https://doi.org/10.1039/C7TA09367E.
49. Khaselev O. High-efficiency integrated multijunction photovoltaic/electrolysis systems for hydrogen production. Int J Hydrogen Energy. 2001;26:127–32. https://doi.org/10.1016/S0360-3199(00)00039-2.
50. Liu C, Tang J, Chen HM, Liu B, Yang P. A fully integrated nanosystem of semiconductor nanowires for direct solar water splitting. Nano Lett. 2013;13:2989–92. https://doi.org/10.1021/nl401615t.
51. Yamane S, Kato N, Kojima S, Imanishi A, Ogawa S, Yoshida N, et al. Efficient solar water splitting with a composite "n-Si/p-CuI/n-i-p a-Si/n-p GaP/RuO_2" semiconductor electrode. J Phys Chem C. 2009;113:14575–81. https://doi.org/10.1021/jp904297v.
52. Higashi T, Kaneko H, Minegishi T, Kobayashi H, Zhong M, Kuang Y, et al. Overall water splitting by photoelectrochemical cells consisting of $(ZnSe)_{0.85}(CuIn_{0.7}Ga_{0.3}Se_2)_{0.15}$ photocathodes and $BiVO_4$ photoanodes. Chem Commun. 2017;53:11674–7. https://doi.org/10.1039/C7CC06637F.
53. Kaneko H, Minegishi T, Nakabayashi M, Shibata N, Kuang Y, Yamada T, et al. A novel photocathode material for sunlight-driven overall water splitting: solid solution of ZnSe and Cu(In, Ga)Se_2. Adv Funct Mater. 2016;26:4570–7. https://doi.org/10.1002/adfm.201600615.
54. Kainthla RC, Zelenay B, Bockris JO. Significant efficiency increase in self-driven photoelectrochemical cell for water photoelectrolysis. J Electrochem Soc. 1987;134:841–5. https://doi.org/10.1149/1.2100583.
55. Brillet J, Cornuz M, Le FF, Yum J-H, Grätzel M, Sivula K. Examining architectures of photoanode–photovoltaic tandem cells for solar water splitting. J Mater Res. 2010;25:17–24. https://doi.org/10.1557/JMR.2010.0009.
56. Kang D, Young JL, Lim H, Klein WE, Chen H, Xi Y, et al. Printed assemblies of GaAs photoelectrodes with decoupled optical and reactive interfaces for unassisted solar water splitting. Nat Energy. 2017;2:17043. https://doi.org/10.1038/nenergy.2017.43.
57. Luo J, Li Z, Nishiwaki S, Schreier M, Mayer MT, Cendula P, et al. Targeting ideal dual-absorber tandem water splitting using perovskite photovoltaics and $CuIn_xGa_{1-x}Se_2$ photocathodes. Adv Energy Mater. 2015;5:1501520. https://doi.org/10.1002/aenm.201501520.

58. Chakthranont P, Hellstern TR, McEnaney JM, Jaramillo TF. Design and fabrication of a precious metal-free tandem core-shell p^+n Si/W-doped $BiVO_4$ photoanode for unassisted water splitting. Adv Energy Mater. 2017;7:1701515. https://doi.org/10.1002/aenm.201701515.
59. Khaselev O, Turner JA. A Monolithic photovoltaic-photoelectrochemical device for hydrogen production via water splitting. Science. 1998;280:425–7. https://doi.org/10.1126/science.280.5362.425.
60. Sun K, Liu R, Chen Y, Verlage E, Lewis NS, Xiang C. A stabilized, intrinsically safe, 10% efficient, solar-driven water-splitting cell incorporating earth-abundant electrocatalysts with steady-state pH gradients and product separation enabled by a bipolar membrane. Adv Energy Mater. 2016;6:1600379. https://doi.org/10.1002/aenm.201600379.
61. Cheng W-H, Richter MH, May MM, Ohlmann J, Lackner D, Dimroth F, et al. Monolithic photoelectrochemical device for direct water splitting with 19% efficiency. ACS Energy Lett. 2018;3:1795–800. https://doi.org/10.1021/acsenergylett.8b00920.
62. Young JL, Steiner MA, Döscher H, France RM, Turner JA, Deutsch TG. Direct solar-to-hydrogen conversion via inverted metamorphic multi-junction semiconductor architectures. Nat Energy. 2017;2:17028. https://doi.org/10.1038/nenergy.2017.28.
63. Verlage E, Hu S, Liu R, Jones RJR, Sun K, Xiang C, et al. A monolithically integrated, intrinsically safe, 10% efficient, solar-driven water-splitting system based on active, stable earth-abundant electrocatalysts in conjunction with tandem III-V light absorbers protected by amorphous TiO_2 films. Energy Environ Sci. 2015;8:3166–72. https://doi.org/10.1039/C5EE01786F.
64. Xu P, Feng J, Fang T, Zhao X, Li Z, Zou Z. Photoelectrochemical cell for unassisted overall solar water splitting using a $BiVO_4$ photoanode and Si nanoarray photocathode. RSC Adv. 2016;6:9905–10. https://doi.org/10.1039/C5RA20115B.
65. Brillet J, Yum J-H, Cornuz M, Hisatomi T, Solarska R, Augustynski J, et al. Highly efficient water splitting by a dual-absorber tandem cell. Nat Photonics. 2012;6:824–8. https://doi.org/10.1038/nphoton.2012.265.
66. Abdi FF, Han L, Smets AHM, Zeman M, Dam B, van de Krol R. Efficient solar water splitting by enhanced charge separation in a bismuth vanadate-silicon tandem photoelectrode. Nat Commun. 2013;4:2195. https://doi.org/10.1038/ncomms3195.
67. Shi X, Jeong H, Oh SJ, Ma M, Zhang K, Kwon J, et al. Unassisted photoelectrochemical water splitting exceeding 7% solar-to-hydrogen conversion efficiency using photon recycling. Nat Commun. 2016;7:11943. https://doi.org/10.1038/ncomms11943.
68. Vijselaar W, Kunturu PP, Moehl T, Tilley SD, Huskens J. Tandem cuprous oxide/silicon microwire hydrogen-evolving photocathode with photovoltage exceeding 1.3 V. ACS Energy Lett. 2019;4:2287–94. https://doi.org/10.1021/acsenergylett.9b01402.
69. Gurudayal, Sabba D, Kumar MH, Wong LH, Barber J, Grätzel M, et al. Perovskite-hematite tandem cells for efficient overall solar driven water splitting. Nano Lett. 2015;15:3833–9. https://doi.org/10.1021/acs.nanolett.5b00616.
70. Koo B, Kim D, Boonmongkolras P, Pae SR, Byun S, Kim J, et al. Unassisted water splitting exceeding 9% solar-to-hydrogen conversion efficiency by Cu(In, Ga)$(S, Se)_2$ photocathode with modified surface band structure and halide perovskite solar cell. ACS Appl Energy Mater. 2020;3:2296–303. https://doi.org/10.1021/acsaem.9b02387.
71. Nam Y, Kim D, Chu J, Park N, Kim TG, Kim KJ, et al. Highly efficient and stable iridium oxygen evolution reaction electrocatalysts based on porous nickel nanotube template enabling tandem devices with solar-to-hydrogen conversion efficiency exceeding 10%. Adv Sci. 2022;9:2104938. https://doi.org/10.1002/advs.202104938.
72. Ingler WB, Khan SUM. A self-driven p/n-Fe_2O_3 tandem photoelectrochemical cell for water splitting. Electrochem Solid State Lett. 2006;9:G144. https://doi.org/10.1149/1.2176082.
73. Lin GH, Kapur M, Kainthla RC, Bockris JO. One step method to produce hydrogen by a triple stack amorphous silicon solar cell. Appl Phys Lett. 1989;55:386–7. https://doi.org/10.1063/1.101879.
74. Moon C, Seger B, Vesborg PCK, Hansen O, Chorkendorff I. Wireless photoelectrochemical water splitting using triple-junction solar cell protected by TiO_2. Cell Reports Phys Sci. 2020;1: 100261. https://doi.org/10.1016/j.xcrp.2020.100261.
75. Calnan S, Aschbrenner S, Bao F, Kemppainen E, Dorbandt I, Schlatmann R. Prospects for hermetic sealing of scaled-up photoelectrochemical hydrogen generators for reliable and risk free operation. Energies. 2019. https://doi.org/10.3390/en12214176.
76. Omrani R, Shabani B. Hydrogen crossover in proton exchange membrane electrolysers: the effect of current density, pressure, temperature, and compression. Electrochim Acta. 2021;377: 138085. https://doi.org/10.1016/j.electacta.2021.138085.
77. Schalenbach M, Carmo M, Fritz DL, Mergel J, Stolten D. Pressurized PEM water electrolysis: efficiency and gas crossover. Int J Hydrogen Energy. 2013;38:14921–33. https://doi.org/10.1016/j.ijhydene.2013.09.013.
78. Rausch B, Symes MD, Chisholm G, Cronin L. Decoupled catalytic hydrogen evolution from a molecular metal oxide redox mediator in water splitting. Science. 2014;345:1326–30. https://doi.org/10.1126/science.1257443.
79. Landman A, Dotan H, Shter GE, Wullenkord M, Houaijia A, Maljusch A, et al. Photoelectrochemical water splitting in separate oxygen and hydrogen cells. Nat Mater. 2017;16:646–51. https://doi.org/10.1038/nmat4876.
80. Hu S, Xiang C, Haussener S, Berger AD, Lewis NS. An analysis of the optimal band gaps of light absorbers in integrated tandem photoelectrochemical water-splitting systems. Energy Environ Sci. 2013;6:2984. https://doi.org/10.1039/c3ee40453f.
81. Döscher H, Geisz JF, Deutsch TG, Turner JA. Sunlight absorption in water—efficiency and design implications for photoelectrochemical devices. Energy Environ Sci. 2014;7:2951–6. https://doi.org/10.1039/C4EE01753F.
82. IEA. World energy outlook 2021. Paris: IEA; 2021.
83. Vesborg PCK, Jaramillo TF. Addressing the terawatt challenge: scalability in the supply of chemical elements for renewable energy. RSC Adv. 2012;2:7933–47. https://doi.org/10.1039/c2ra20839c.
84. Battaglia C, Cuevas A, De Wolf S. High-efficiency crystalline silicon solar cells: status and perspectives. Energy Environ Sci. 2016;9:1552–76. https://doi.org/10.1039/c5ee03380b.
85. van de Krol R, Liang Y. An n-Si/n-Fe_2O_3 heterojunction tandem photoanode for solar water splitting. Chim Int J Chem. 2013;67:168–71. https://doi.org/10.2533/chimia.2013.168.
86. Sivula K, Van De Krol R. Semiconducting materials for photoelectrochemical energy conversion. Nat Rev Mater. 2016. https://doi.org/10.1038/natrevmats.2015.10.
87. Austin IG, Mott NF. Metallic and nonmetallic behavior in transition metal oxides. Science. 1970;168:71–7. https://doi.org/10.1126/science.168.3927.71.
88. Rettie AJE, Chemelewski WD, Emin D, Mullins CB. Unravelling small-polaron transport in metal oxide photoelectrodes. J Phys Chem Lett. 2016;7:471–9. https://doi.org/10.1021/acs.jpclett.5b02143.

89. Corby S, Rao RR, Steier L, Durrant JR. The kinetics of metal oxide photoanodes from charge generation to catalysis. Nat Rev Mater. 2021;6:1136–55. https://doi.org/10.1038/s41578-021-00343-7.
90. Xia C, Wang H, Kim JK, Wang J. Rational design of metal oxide-based heterostructure for efficient photocatalytic and photoelectrochemical systems. Adv Funct Mater. 2021;31:1–31. https://doi.org/10.1002/adfm.202008247.
91. Rohloff M, Anke B, Zhang S, Gernert U, Scheu C, Lerch M, et al. Mo-doped $BiVO_4$ thin films-high photoelectrochemical water splitting performance achieved by a tailored structure and morphology. Sustain Energy Fuels. 2017;1:1830–46. https://doi.org/10.1039/c7se00301c.
92. Zandi O, Klahr BM, Hamann TW. Highly photoactive Ti-doped α-Fe_2O_3 thin film electrodes: resurrection of the dead layer. Energy Environ Sci. 2013;6:634–42. https://doi.org/10.1039/c2ee23620f.
93. Concina I, Ibupoto ZH, Vomiero A. Semiconducting metal oxide nanostructures for water splitting and photovoltaics. Adv Energy Mater. 2017;7:1–29. https://doi.org/10.1002/aenm.201700706.
94. Al-Ashouri A, Köhnen E, Li B, Magomedov A, Hempel H, Caprioglio P, et al. Monolithic perovskite/silicon tandem solar cell with > 29% efficiency by enhanced hole extraction. Science. 2020;370:1300–9. https://doi.org/10.1126/science.abd4016.
95. Reece SY, Hamel JA, Sung K, Jarvi TD, Esswein AJ, Pijpers JJH, et al. Wireless solar water splitting using silicon-based semiconductors and earth-abundant catalysts. Science. 2011;334:645–8. https://doi.org/10.1126/science.1209816.
96. Bae D, Seger B, Vesborg PCK, Hansen O, Chorkendorff I. Strategies for stable water splitting: via protected photoelectrodes. Chem Soc Rev. 2017;46:1933–54. https://doi.org/10.1039/c6cs00918b.
97. Mei B, Pedersen T, Malacrida P, Bae D, Frydendal R, Hansen O, et al. Crystalline TiO_2: a generic and effective electron-conducting protection layer for photoanodes and -cathodes. J Phys Chem C. 2015;119:15019–27. https://doi.org/10.1021/acs.jpcc.5b04407.
98. Cui W, Moehl T, Siol S, Tilley SD. Operando electrochemical study of charge carrier processes in water splitting photoanodes protected by atomic layer deposited TiO_2. Sustain Energy Fuels. 2019;3:3085–92. https://doi.org/10.1039/C9SE00399A.
99. Nunez P, Richter MH, Piercy BD, Roske CW, Cabán-Acevedo M, Losego MD, et al. Characterization of electronic transport through amorphous TiO_2 produced by atomic layer deposition. J Phys Chem C. 2019;123:20116–29. https://doi.org/10.1021/acs.jpcc.9b04434.
100. Hu S, Shaner MR, Beardslee JA, Lichterman M, Brunschwig BS, Lewis NS. Amorphous TiO_2 coatings stabilize Si, GaAs, and GaP photoanodes for efficient water oxidation. Science. 2014;344:1005–9. https://doi.org/10.1126/science.1251428.
101. Irwin MD, Buchholz DB, Hains AW, Chang RPH, Marks TJ. p-Type semiconducting nickel oxide as an efficiency-enhancing anode interfacial layer in polymer bulk-heterojunction solar cells. Proc Natl Acad Sci U S A. 2008;105:2783–7. https://doi.org/10.1073/pnas.0711990105.
102. Kim IS, Pellin MJ, Martinson ABF. Acid-compatible halide perovskite photocathodes utilizing atomic layer deposited TiO_2 for solar-driven hydrogen evolution. ACS Energy Lett. 2019;4:293–8. https://doi.org/10.1021/acsenergylett.8b01661.
103. Bae D, Pedersen T, Seger B, Iandolo B, Hansen O, Vesborg PCK, et al. Carrier-selective p- and n-contacts for efficient and stable photocatalytic water reduction. Catal Today. 2017;290:59–64. https://doi.org/10.1016/j.cattod.2016.11.028.
104. McDowell MT, Lichterman MF, Carim AI, Liu R, Hu S, Brunschwig BS, et al. The influence of structure and processing on the behavior of TiO_2 protective layers for stabilization of n-Si/TiO_2/Ni photoanodes for water oxidation. ACS Appl Mater Interfaces. 2015;7:15189–99. https://doi.org/10.1021/acsami.5b00379.
105. Ros C, Carretero NM, David J, Arbiol J, Andreu T, Morante JR. Insight into the degradation mechanisms of atomic layer deposited TiO_2 as photoanode protective layer. ACS Appl Mater Interfaces. 2019;11:29725–35. https://doi.org/10.1021/acsami.9b05724.
106. Seger B, Tilley DS, Pedersen T, Vesborg PCK, Hansen O, Grätzel M, et al. Silicon protected with atomic layer deposited TiO_2: durability studies of photocathodic H_2 evolution. RSC Adv. 2013;3:25902. https://doi.org/10.1039/c3ra45966g.
107. Yamaguchi M, Dimroth F, Geisz JF, Ekins-Daukes NJ. Multi-junction solar cells paving the way for super high-efficiency. J Appl Phys. 2021;129: 240901. https://doi.org/10.1063/5.0048653.
108. Horowitz KAW, Remo T, Smith B, Ptak A. A techno-economic analysis and cost reduction roadmap for 3–5 solar cells. Golden: National Renewable Energy Laboratory; 2018.
109. Tembhurne S, Nandjou F, Haussener S. A thermally synergistic photo-electrochemical hydrogen generator operating under concentrated solar irradiation. Nat Energy. 2019;4:399–407. https://doi.org/10.1038/s41560-019-0373-7.
110. Shaner MR, Atwater HA, Lewis NS, McFarland EW. A comparative technoeconomic analysis of renewable hydrogen production using solar energy. Energy Environ Sci. 2016;9:2354–71. https://doi.org/10.1039/c5ee02573g.
111. Pinaud BA, Benck JD, Seitz LC, Forman AJ, Chen Z, Deutsch TG, et al. Technical and economic feasibility of centralized facilities for solar hydrogen production via photocatalysis and photoelectrochemistry. Energy Environ Sci. 2013;6:1983–2002. https://doi.org/10.1039/c3ee40831k.
112. Wang Z, Gu Y, Wang L. Revisiting solar hydrogen production through photovoltaic-electrocatalytic and photoelectrochemical water splitting. Front Energy. 2021;15:596–9. https://doi.org/10.1007/s11708-021-0745-0.